2013

Acoustically assisted spin-transfer-torque switching of nanomagnets: An energy-efficient hybrid writing scheme for non-volatile memory

Ayan K. Biswas
Virginia Commonwealth University, biswasak@vcu.edu

Supriyo Bandyopadhyay
Virginia Commonwealth University, sbandy@vcu.edu

Jayasimha Atulasimha
Virginia Commonwealth University, jatulasimha@vcu.edu

Biswas, A.K., Bandyopadhyay, S., Atulasimha, J. Acoustically assisted spin-transfer-torque switching of nanomagnets: An energy-efficient hybrid writing scheme for non-volatile memory. Applied Physics Letter, 103, 232401 (2013).

APPLIED PHYSICS LETTERS **103**, 232401 (2013)

Acoustically assisted spin-transfer-torque switching of nanomagnets: An energy-efficient hybrid writing scheme for non-volatile memory

Ayan K. Biswas,[1] Supriyo Bandyopadhyay,[1] and Jayasimha Atulasimha[2]
[1]*Department of Electrical and Computer Engineering, Virginia Commonwealth University, Richmond, Virginia 23284, USA*
[2]*Department of Mechanical and Nuclear Engineering, Virginia Commonwealth University, Richmond, Virginia 23284, USA*

(Received 27 September 2013; accepted 17 November 2013; published online 2 December 2013)

We show that the energy dissipated to write bits in spin-transfer-torque random access memory can be reduced by an order of magnitude if a surface acoustic wave (SAW) is launched underneath the magneto-tunneling junctions (MTJs) storing the bits. The SAW-generated strain rotates the magnetization of every MTJs' soft magnet from the easy towards the hard axis, whereupon passage of a small spin-polarized current through a target MTJ selectively switches it to the desired state with $>99.99\%$ probability at room temperature, thereby writing the bit. The other MTJs return to their original states at the completion of the SAW cycle. © *2013 AIP Publishing LLC*.
[http://dx.doi.org/10.1063/1.4838661]

Switching the magnetization of soft nanomagnets with spin transfer torque (STT) generated from a spin polarized current has been a popular approach to write bits in non-volatile magnetic memory implemented with magneto-tunneling junctions (MTJ).[1–3] However, this mode of switching is energy-inefficient and consumes much more energy than is needed to switch transistors. Recently, we have shown that it is possible to rotate the magnetization of a strain-coupled magnetostrictive-piezoelectric (multiferroic) nanomagnet possessing uniaxial shape-anisotropy by a large angle ($\sim 90^\circ$) with a small voltage applied to the piezoelectric layer. The voltage generates strain in the piezoelectric layer, which is transferred to the magnetostrictive layer and rotates its magnetization, while dissipating very little energy.[4–6] Such rotations have also been demonstrated experimentally in multi-domain thin films.[7–9] Although it is remarkably energy-efficient, this mode of switching unfortunately allows rotation of the magnetization by only up to 90° in isolated magnets, which does not result in a magnetization flip. When the voltage is later turned off, the magnetization will relax to one of the two stable orientations along the easy axis with equal probability, thus resulting in a $\sim 50\%$ chance of flip (i.e., 50% chance of writing the bit correctly), which is unacceptable. The flip probability can be increased dramatically to over 99% at room temperature by rapidly turning the voltage off at the precise juncture when the magnetization vector subtends an angle of 90° with the easy axis,[10] but that approach requires complex pulse shaping and/or feedback circuitry which are at least unattractive, if not impractical. An alternate approach is a hybrid one: strain a magnetostrictive magnet with a surface acoustic wave (SAW) flowing underneath it and synchronously inject a small spin polarized current during the appropriate cycle of the SAW to drive the magnetization to the desired orientation. This does not require complex pulse shaping or feedback circuitry. Two conditions however must be fulfilled for reliability: (1) the probability of switching the magnetization of a magnet to the desired orientation (writing of bits) must be $\sim 100\%$ at room temperature when the small spin-polarized current is injected, and (2) the probability of unintentionally switching the magnet due to the SAW alone is $\sim 0\%$ at room temperature when no spin-polarized current is injected. This will ensure that bits are written reliably in the target memory cells and data already stored in other cells are not corrupted. We show that both conditions can be fulfilled with proper design.

The concept of using a SAW to rotate magnetization of magnets is not new. Magnetization precession due to picosecond acoustic strain pulse has been studied for weakly magnetostrictive materials like GaMnAs[11,12] and Ni.[13] A very recent theoretical paper[14] examined picosecond acoustic pulse-induced rotation of in-plane magnetization in the magnetostrictive material Terfenol-D. Another study focused on using a Rayleigh wave (SAW) to generate strain in a cubic crystal and thus switch the magnetization of a perpendicularly magnetized (Ga, Mn)(As, P) layer elastically coupled with the crystal.[15] However, all of these studies ignored thermal fluctuations that are present at non-zero temperatures. Magnetization dynamics is extremely vulnerable to thermal noise and their influence cannot be overlooked. In this letter, we have studied hybrid switching of magnetization with SAW and STT taking into account random thermal noise at room temperature.

We consider a magnetostrictive Terfenol-D nanomagnet, shaped like an elliptical cylinder, resting on a piezoelectric substrate, whose cross-section lies in the y-z plane. The major axis is along the z-direction and the minor axis is along the y-direction (Figure 1). The major axis $a = 110$ nm, the minor axis $b = 90$ nm, and the thickness $d = 7$ nm. These dimensions ensure that the magnet has but a single domain[16] and that the shape anisotropy energy barrier is 2.2 eV (85.12 kT at room temperature), which makes the probability of spontaneous magnetization flipping due to thermal agitations equal to e^{-85} per attempt.[17] Therefore, the memory retention time is $(1/f_0)\, e^{85} = 2.6 \times 10^{17}$ years, if we assume the attempt frequency f_0 to be 1 THz.[18]

Figure 1 shows the complete system consisting of a $LiNbO_3$ piezoelectric substrate on which interdigital

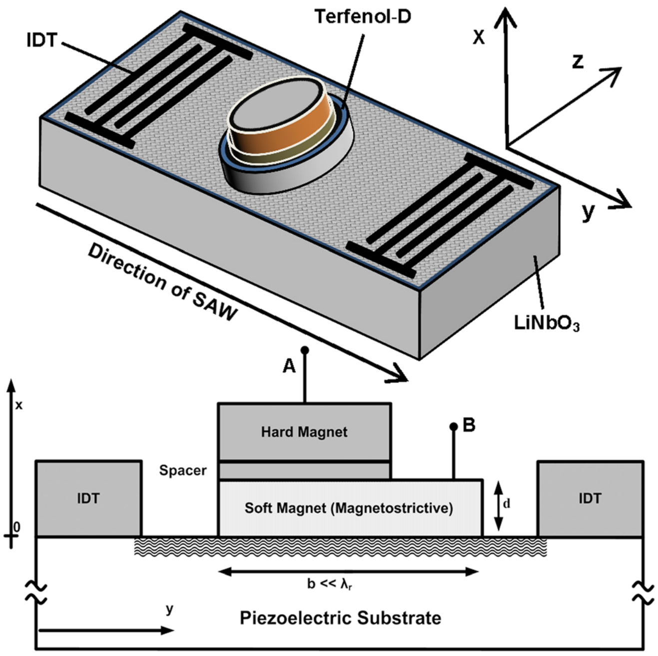

FIG. 1. (Top) Schematic illustration of the system with IDTs and a MTJ, serving as a bit storage unit, placed between IDTs on a *LiNbO*$_3$ piezoelectric substrate. The soft layer of the MTJ is in contact with the substrate and is strained by the SAW. The resistance between the terminals A and B is used to read the bit stored (we assume that both magnets are metallic). For writing, a small spin polarized current is passed between the same two terminals during the appropriate cycle of the SAW. In this configuration, the reading and writing currents do not pass through the highly resistive piezoelectric, so the dissipation during the read/write operation is kept small. Bits are addressed for read/write using the traditional crossbar architecture.

transducers (IDT) are delineated for launching a SAW. The magnet is placed between the IDT fingers. A SAW wave of frequency 100 MHz is launched and propagates along the y-direction with velocity $v_r = 3488$ m/s in *LiNbO*$_3$.[19] The corresponding wavelength λ_r is 34.88 μm. We assume the SAW mode to be a Rayleigh wave that has three strain components: a tangential component along the y-direction, a normal component along the x-direction, and a shear component in the x-y plane. Since $b \ll \lambda_r$, we can consider the strain to be uniformly distributed across the magnet. We also neglect any shear lag effect since the magnet's thickness is much smaller than its lateral dimensions. Furthermore, since $d \ll \lambda_r$, shear has no effect.[15] Finally, since the top of the magnet is not clamped, we can neglect the normal component of stress. Therefore, we need to consider only a uniaxial tangential component along the y-direction, i.e., the hard axis of the magnet. We can also assume that the strain generated in the magnet is equal to the surface strain on the piezoelectric substrate since $d \ll \lambda_r$.[20]

We will assume that the nanomagnet is polycrystalline and hence there is no magnetocrystalline effect to consider. In that case, the potential energy of the magnet at any instant of time t is given by

$$
\begin{aligned}
E(t) &= E_{ss}(t)\sin^2\theta(t) + \frac{\mu_0}{2}\Omega M_s^2 N_{d-zz},\\
E_{ss}(t) &= \left(\frac{\mu_0}{2}\right)\Omega M_s^2\{N_{d-xx}\cos^2\phi(t) + N_{d-yy}\sin^2\phi(t)\\
&\quad - N_{d-zz}\} - \frac{3}{2}\lambda_s\epsilon(t)Y\Omega\sin^2\phi(t),
\end{aligned}
\tag{1}
$$

where $\theta(t)$ and $\phi(t)$ are, respectively, the instantaneous polar and azimuthal angles of the magnetization vector, M_s is the saturation magnetization of Terfenol-D, N_{d-xx}, N_{d-yy}, and N_{d-zz} are the demagnetization factors that can be evaluated from the magnet's dimensions,[21] μ_0 is the permeability of free space, $\Omega = (\pi/4)abd$ is the magnet's volume, λ_s is the magnetostriction coefficient, Y is the Young's modulus, and $\epsilon(t)$ is the strain generated by the SAW at the instant of time t. The last quantity is determined by the launched SAW power, beam width and frequency.[20]

The torque on the magnetization vector at any time t due to shape- and stress-anisotropy can be expressed as

$$
\begin{aligned}
\tau_{ss}(t) &= -\mathbf{m}(t)\times\left(\frac{\partial E}{\partial\theta(t)}\hat{\boldsymbol{\theta}} + \frac{1}{\sin\theta(t)}\frac{\partial E}{\partial\phi(t)}\hat{\boldsymbol{\phi}}\right),\\
&= E_{\phi s}(t)\sin\theta(t)\hat{\boldsymbol{\theta}} - E_{ss}(t)\sin 2\theta(t)\hat{\boldsymbol{\phi}},
\end{aligned}
\tag{2}
$$

where $\mathbf{m}(t)$ is the normalized magnetization vector and $E_{\phi s}(t) = \left\{\frac{\mu_0}{2}M_s^2(N_{d-yy} - N_{d-xx}) - \frac{3}{2}\lambda_s\epsilon(t)Y\right\}\Omega\sin 2\phi(t)$.

During one half-cycle of the SAW, the stress generated on the magnetostrictive layer is compressive and during the other half, it is tensile. The magnetization rotates towards the hard axis during one of these half-cycles (depending on the sign of the magnetostriction coefficient) and during the *latter half* of that half-cycle (after the magnetization has already rotated substantially because of the stress), a spin-polarized current is passed through the magnet to rotate the magnetization by $\sim 180°$. Thus, the current lasts for only a quarter cycle of the SAW (see the inset of Fig. 2). Passage of the spin polarized current I_s through the nanomagnet generates a spin transfer torque on the magnetization vector given by[22]

$$
\tau_{sst}(t) = s[\mathsf{b}\sin(\zeta - \theta(t))\hat{\boldsymbol{\phi}} - \mathsf{c}\sin(\zeta - \theta(t))\hat{\boldsymbol{\theta}}],
\tag{3}
$$

where $s = (\hbar/2e)\eta I_s$ is the spin angular deposition per unit time, η is the spin polarization of the current, b and c are coefficients of the out-of-plane and in-plane components of the spin-transfer-torque. The current is passed perpendicular to the plane of the magnet. The quantity ζ is the angle

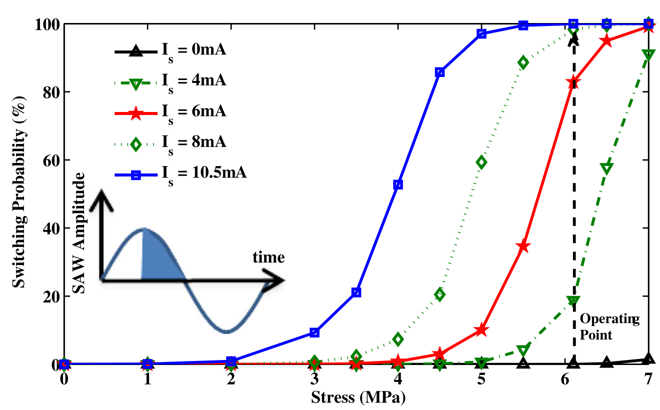

FIG. 2. Probability of a magnet switching at room temperature in 5 ns (half-period of the 100 MHz SAW) as a function of the peak stress generated by the SAW. The various curves are for different spin-polarized currents. Note that the probability of switching in the absence of spin polarized current remains zero up to a peak stress of 6.1 MPa. The spin-polarized current is turned on for the latter half of the appropriate half-cycle of the SAW (2.5 ns) as shown in the inset (shaded region) to write the bit.

subtended by the direction of spin polarization with the z-axis and we assume it to be zero.

At non-zero temperatures, thermal noise generates a random magnetic field $\mathbf{h}(t)$ given by[17]

$$\mathbf{h}(t) = h_x(t)\hat{\boldsymbol{x}} + h_y(t)\hat{\boldsymbol{y}} + h_z(t)\hat{\boldsymbol{z}}. \tag{4}$$

The components of $\mathbf{h}(t)$ are[23] $h_i(t) = \sqrt{\frac{2\alpha kT}{|\gamma|(1+\alpha^2)\mu_0 M_s \Omega \Delta t}}\, N_{(0,1)}(t)$; $(i = x, y, z)$. Here, α is the dimensionless Gilbert damping constant for Terfenol-D, γ is the gyromagnetic ratio for electrons, and Δt is a quantity that is inversely proportional to the attempt frequency of the thermal field to perturb the magnetization. The quantity $N_{(0,1)}(t)$ is a Gaussian with zero mean and unit standard deviation.[24]

The random thermal field gives rise to a random thermal torque that can be expressed as[25]

$$\tau_{\mathbf{th}}(t) = \mu_0 M_s \Omega \mathbf{m}(t) \times \mathbf{h}(t) = -\mu_0 M_s \Omega [h_\phi(t)\hat{\boldsymbol{\theta}} - h_\theta(t)\hat{\boldsymbol{\phi}}],$$

where

$$\begin{aligned} h_\theta(t) &= h_x \cos\theta(t)\cos\phi(t) + h_y \cos\theta(t)\sin\phi(t) - h_z \sin\theta(t), \\ h_\phi(t) &= -h_x \sin\phi(t) + h_y \cos\phi(t). \end{aligned} \tag{5}$$

In order to find the temporal evolution of the magnetization vector under the three different torques mentioned above, we solve the stochastic Landau-Lifshitz-Gilbert (LLG) equation under the macrospin assumption

$$\begin{aligned} &\frac{d\mathbf{m}(t)}{dt} - \alpha\left(\mathbf{m}(t) \times \frac{d\mathbf{m}(t)}{dt}\right) \\ &\quad = \frac{-|\gamma|}{\mu_0 M_s \Omega}\left(\tau_{\mathbf{ss}}(t) + \tau_{\mathbf{th}}(t) + \tau_{\mathbf{sst}}(t)\right). \end{aligned} \tag{6}$$

From the above equation, we can derive two coupled equations for the temporal evolution of the polar and azimuthal angles of the magnetization vector

$$\begin{aligned} \theta'(t) = &-\frac{|\gamma|}{(1+\alpha^2)\mu_0 M_s \Omega}\{E_{\phi s}\sin\theta(t) - \mu_0 M_s \Omega h_\phi(t) \\ &+ s\mathsf{c}\sin\theta(t) + \alpha(E_{ss}\sin 2\theta(t) \\ &+ s\mathsf{b}\sin\theta(t) - \mu_0 M_s \Omega h_\theta(t))\}, \end{aligned} \tag{7}$$

$$\begin{aligned} \phi'(t) = &\frac{|\gamma|}{\sin\theta(t)(1+\alpha^2)\mu_0 M_s \Omega}\{E_{ss}\sin 2\theta(t) \\ &+ s\mathsf{b}\sin\theta(t) - \mu_0 M_s \Omega h_\theta(t) - \alpha(E_{\phi s}\sin\theta(t) \\ &+ s\mathsf{c}\sin\theta(t) - \mu_0 M_s \Omega h_\phi(t))\}, \end{aligned} \tag{8}$$

where the "prime" denotes time-derivative.

We assume the following material parameters for Terfenol-D: Saturation magnetization $M_s = 8 \times 10^5$ A/m, magnetostriction coefficient $(3/2)\lambda_s = 90 \times 10^{-5}$, Young's modulus $Y = 80$ GPa, and Gilbert damping coefficient $\alpha = 0.1$.[26–28] For the spin transfer torque, we assume the following parameters: $\mathsf{b} = 0.3$, $\mathsf{c} = 1.0$, and spin polarization $\eta = 0.3$.

To simulate magnetization flipping due to strain and STT in the presence of thermal fluctuations, we simulate 10 000 switching trajectories, each lasting for one-half cycle of the SAW (5 ns). For each trajectory, the initial orientation of the magnetization vector is picked from the thermal distribution around the -z-axis. We then simulate a switching trajectory by solving the stochastic Eqs. (7) and (8) to find the values of $\theta(t)$ and $\phi(t)$ at time intervals of 10^{-13} s. We terminate each switching trajectory (terminate simulation) at the end of 5 ns. We verify that each trajectory ends up with a final value of θ that is either $<5°$ or $>175°$ after completion of the SAW half-cycle (5 ns). In the next half-cycle, the stress changes sign and tends to drive the magnetization even more towards the easy axis, so this half-cycle need not be considered in the simulation. The final state $\theta_{final} \leq 5°$ implies switching success and $\theta_{final} \geq 175°$ implies switching failure. The fraction of switching trajectories out of 10 000 that results in switching success is the switching probability.

In Fig. 2, we plot the switching probability at room temperature as a function of peak stress generated by the SAW for various spin-polarized currents. If no spin-polarized current is present, then the probability remains $<0.01\%$ for peak stresses up to 6.1 MPa. This has an important implication. Note that the SAW is "global" and affects every memory cell. Specificity, i.e., which particular cell is written into, is implemented by ensuring that the SAW *alone* cannot flip the magnetization of the magnetostrictive layer, and that *both* SAW and STT are required for a flip. Therefore, *only* those cells into which a spin polarized current is injected can switch to the desired state, while the others remain unswitched. This ensures that data stored in unaddressed cells are not corrupted. We then find the minimum spin-polarized current that is required to switch the addressed cells with $>99.99\%$ probability, while the SAW parameters are kept such that the peak stress generated in every cell is equal to the critical stress of 6.1 MPa. We find from Fig. 2, that this current is 10.5 mA. We have also found that if we switch using STT alone (stress = 0), then the minimum current required to switch with $>99.99\%$ probability at room temperature is 23 mA, provided we pass it for the entire half-cycle of 5 ns (and not just the quarter cycle of 2.5 ns). Thus, by adopting the hybrid switching scheme (STT + SAW), we have reduced the write current by a factor of 2.2 and the current duration by a factor of 2.

Note that in the absence of any spin polarized current, the probability of switching a magnet in 5 ns with SAW alone is $<0.01\%$ as long as the peak stress is kept at or below 6.1 MPa. This ensures that unaddressed cells are not corrupted by the SAW.

The energy dissipated to switch a magnet in the hybrid scheme has three contributions:[20] energy dissipated in the magnet due to Gilbert damping, energy dissipated in the SAW, and the energy dissipated by the spin-polarized STT current. For a SAW beam width of 5 μm and frequency 100 MHz (half cycle = 5 ns), the SAW power required to generate a peak stress of 6.1 MPa is 187.5 μW,[20] but it is amortized over all the magnets affected by the SAW and hence is a negligible quantity per magnet. The overwhelmingly dominant contribution to the dissipation is the $I_s^2 R t_s$ loss,[20] where I_s is the STT current, R is the resistance of the MTJ stack through which the current flows, and t_s is the quarter cycle time (2.5 ns). In Ref. 29, the specific resistance of a fabricated MTJ stack was reported to be between 0.5 and 10 $\Omega\ \mu m^2$. For our dimensions, this translates to a resistance of 64.3 Ω, if we take the lower value.

In Fig. 3, we plot the total energy dissipated to switch a magnet (and hence write a bit) with > 99.99% probability, using both STT and SAW, as a function of the peak stress generated by the SAW. Note that the energy dissipation decreases by nearly an order of magnitude when we adopt the hybrid scheme (STT + SAW) and operate at the maximum stress level of 6.1 MPa, as opposed to the STT-alone scheme (stress = 0). This happens because the SAW helps to rotate the magnetization and therefore decreases the STT current needed to switch by a factor of 2.2. At the same time, it also decreases the current flow duration by a factor of 2. The absolute value of the energy dissipation in the hybrid mode can be decreased further with appropriate material choice for the magnetostrictive magnet (materials with lower saturation magnetization but not much lower magnetostriction coefficient).[30]

An important question that may arise is why one needs to use a SAW instead of just straining the magnets with local electrostatic potentials by exploiting the d_{33} or d_{31} coupling in $LiNbO_3$. Such an approach was proposed in Ref. 31, which carried out LLG simulations at 0 K, without thermal perturbations, and also neglected the out-of-plane motion of the magnetization vector. Applying local potentials however will require electrically contacting every magnet, which adds an additional layer of fabrication complexity that is not needed. The SAW propagates through the entire substrate and strains every magnet periodically without requiring an electrical contact to each magnet. This relieves the associated lithography burden. Of course, local connections could also be avoided by applying a potential across the entire wafer (with a back-gate) to stress all the magnets simultaneously. However, this approach is impractical since the electric field needed to generate a stress of, say, 4 MPa in the Terfenol-D layer of a nanomagnet is ~8.1 MV/m (d_{31} of $LiNbO_3 = 6 \times 10^{-12}$ m/V). We cannot grow a thin film of $LiNbO_3$ on a conducting substrate since the substrate will clamp the film and prevent it from being strained. Therefore, we must work with a $LiNbO_3$ substrate, which must be at least 1 mm thick for mechanical sturdiness. Consequently, the voltage required to strain the entire wafer will be 8.1 kV, which is clearly prohibitive.

In conclusion, we have shown that hybrid mode switching (STT + SAW) can be more energy-efficient than switching with STT alone. The hybrid scheme is therefore an attractive methodology to write bits in spin-transfer-torque memory.

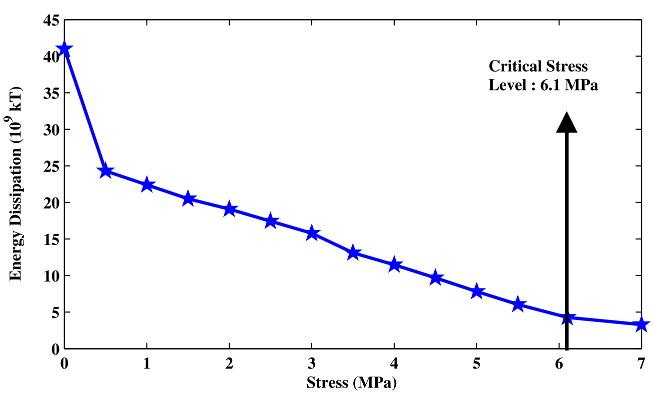

FIG. 3. Energy dissipated to switch a magnet in the hybrid mode with > 99.99% probability in 5 ns as a function of peak stress generated by the SAW. The safe stress level is ≤ 6.1 MPa.

All authors acknowledge support from the National Science Foundation (NSF) under the NEB2020 Grant No. ECCS-1124714 and SHF Grant No. CCF-1216614 as well as the Semiconductor Research Company (SRC) under NRI task 2203.001. J. Atulasimha acknowledges support from NSF CAREER Grant No. CCF-1253370.

[1] J. Slonczewski, J. Magn. Magn. Mater. **159**, L1 (1996).
[2] H. Kubota, A. Fukushima, K. Yakushiji, T. Nagahama, S. Yuasa, K. Ando, H. Maehara, Y. Nagamine, K. Tsunekawa, D. D. Djayaprawira, N. Watanabe, and Y. Suzuki, Nat. Phys. **4**, 37 (2008).
[3] D. C. Ralph and M. D. Stiles, J. Magn. Magn. Mater. **320**, 1190 (2008).
[4] J. Atulasimha and S. Bandyopadhyay, Appl. Phys. Lett. **97**, 173105 (2010).
[5] K. Roy, S. Bandyopadhyay, and J. Atulasimha, Appl. Phys. Lett. **99**, 063108 (2011).
[6] M. S. Fashami, K. Roy, J. Atulasimha, and S. Bandyopadhyay, Nanotechnology **22**, 155201 (2011).
[7] T. Brintlinger, S.-H. Lim, K. H. Baloch, P. Alexander, Y. Qi, J. Barry, J. Melngailis, L. Salamanca-Riba, I. Takeuchi, and J. Cumings, Nano Lett. **10**, 1219 (2010).
[8] D. E. Parkes, S. A. Cavill, A. T. Hindmarch, P. Wadley, F. McGee, C. R. Staddon, K. W. Edmonds, R. P. Campion, B. L. Gallagher, and A. W. Rushforth, Appl. Phys. Lett. **101**, 072402 (2012).
[9] C.-J. Hsu, J. L. Hockel, and G. P. Carman, Appl. Phys. Lett. **100**, 092902 (2012).
[10] K. Roy, S. Bandyopadhyay, and J. Atulasimha, Nature Sci. Rep. **3**, 3038 (2013).
[11] A. Scherbakov, A. S. Salasyuk, A. Akimov, X. Liu, M. Bombeck, C. Brüggemann, D. R. Yakovlev, V. F. Sapega, J. K. Furdyna, and M. Bayer, Phys. Rev. Lett. **105**, 117204 (2010).
[12] L. Thevenard, E. Peronne, C. Gourdon, C. Testelin, M. Cubukcu, E. Charron, S. Vincent, A. Lemaître, and B. Perrin, Phys. Rev. B **82**, 104422 (2010).
[13] J.-W. Kim, M. Vomir, and J.-Y. Bigot, Phys. Rev. Lett. **109**, 166601 (2012).
[14] O. Kovalenko, T. Pezeril, and V. V. Temnov, Phys. Rev. Lett. **110**, 266602 (2013).
[15] L. Thevenard, J.-Y. Duquesne, E. Peronne, H. J. von Bardeleben, H. Jaffres, S. Ruttala, J.-M. George, A. Lemaître, and C. Gourdon, Phys. Rev. B **87**, 144402 (2013).
[16] R. P. Cowburn, D. K. Koltsov, A. O. Adeyeye, M. E. Welland, and D. M. Tricker, Phys. Rev. Lett. **83**, 1042 (1999).
[17] W. F. Brown, Jr., Phys. Rev. **130**, 1677 (1963).
[18] P. Gaunt, J. Appl. Phys. **48**, 3470 (1977).
[19] A. J. Slobodnik, E. D. Conway, and R. T. Delmonico, *Microwave Acoustic Handbook* (AFCRL Report No. 73-0597, Air Force Cambridge Research Laboratories, Bedford, Massachusetts, 1973), Vol. 1A, p. 402.
[20] See supplementary material at http://dx.doi.org/10.1063/1.4838661 for detailed derivations of strain and of energy dissipation.
[21] S. Chikazumi, *Physics of Magnetism* (Wiley, New York, 1964).
[22] S. Salahuddin, D. Datta, and S. Datta, e-print arXiv:0811.3472 [cond-mat.mes-hall].
[23] B. Behin-Aein, D. Datta, S. Salahuddin, and S. Datta, Nat. Nanotechnol. **5**, 266 (2010).
[24] G. Brown, M. A. Novotny, and P. A. Rikvold, Phys. Rev. B **64**, 134422 (2001).
[25] K. Roy, S. Bandyopadhyay, and J. Atulasimha, J. Appl. Phys. **112**, 023914 (2012).
[26] R. Abbundi and A. E. Clark, IEEE Trans. Magn. **13**, 1519 (1977).
[27] K. Ried, M. Schnell, F. Schatz, M. Hirscher, B. Ludescher, W. Sigle, and H. Kronmüller, Phys. Status Solidi A **167**, 195 (1998).
[28] R. Kellogg and A. Flatau, J. Intell. Mater. Syst. Struct. **19**, 583 (2008).
[29] Y. Huai, F. Albert, P. Nguyen, M. Pakala, and T. Valet, Appl. Phys. Lett. **84**, 3118 (2004).
[30] G. E. Rowlands, T. Rahman, J. A. Katine, J. Langer, A. Lyle, H. Zhao, J. G. Alzate, A. A. Kovalev, Y. Tserkovnyak, Z. M. Zeng, H. W. Jiang, K. Galatsis, Y. M. Huai, P. K. Amiri, K. L. Wang, I. N. Krivorotov, and J.-P. Wang, Appl. Phys. Lett. **98**, 102509 (2011).
[31] K. Roy, S. Bandyopadhyay, and J. Atulasimha, e-print arXiv:1012.0819 [cond-mat.mes-hall].